CONF-8706113--3

CLOSE COLLISIONS BETWEEN LIGHT NUCLEI - ORBITING AND FUSION

D. Shapira
Physics Division, Oak Ridge National Laboratory*
Oak Ridge, TN 37831 USA

B. Shivakumar
A. W. Wright Nuclear Structure Laboratory, Yale University
New Haven, CT 06511 USA

B. A. Harmon
University of Virginia
Charlottesville, VA 22901 USA

and

S. Ayik
Tennessee Technological University
Cookeville, TN 38505 USA

CONF-8706113--3

DE87 011178

INTRODUCTION

In close collisions, nuclear matter, energy and angular momentum undergo substantial rearrangement. Studies of such processes should enhance our understanding of the nuclear many-body system and of the behavior of bulk nuclear matter, and the interesting results and models based on such data for heavy nuclei bear this out [1]. The lighter nuclei, on which this study focuses, are unique in several respects: the binding energy per nucleon increases with mass number for these nuclei - therefore the amalgamation of two such nuclei produces a composite at high excitation energies even for relatively low bombarding energies. Fission of light nuclei ($A < 80$) into two complex fragments is also severely restricted for that reason. In these light systems the Coulomb and centrifugal barriers can attain comparable magnitude and both barriers influence the outcome of the collision. Finally, the study of collisions between light nuclei affords the experimenter with the possibility of full identification of all the detected reaction products, with modest efforts - and none was

*Operated by Martin Marietta Energy Systems, Inc. under contract DE-AC05-84OR21400 with the U.S. Department of Energy.

spared in obtaining the high quality data that will be presented.

Our data have demonstrated that in close collisions the two nuclei first form a rotating dinuclear complex (DNC) which can break up into two complex fragments (Orbiting) or evolve into a compound nucleus. The binary fragment yield was found to be significant in contradiction with earlier views which held that whenever nucleus-nucleus capture occurs fusion is a certainty [2]. The time duration of the dinuclear stage and the nature of its evolution into a compound nucleus were studied and a model which describes these processes will be presented.

ORBITING DATA

Where one might find the yield from nuclear orbiting is shown in Fig. 1 which appeared in an article written by Wilczyński 15 years ago [3]. We have chosen to look at backward angles, near 180 degrees, where such fully damped products appear isolated. The study of reaction products at backward angles was facilitated by using a combination of a heavier beam with a light target and studying target-like recoils at forward angles ('reverse kinematics'). The results from such measurements confirm the existence of large yields of fully damped fragments from a binary process [4,5]. Typical Q-value spectra for carbons emitted at backward

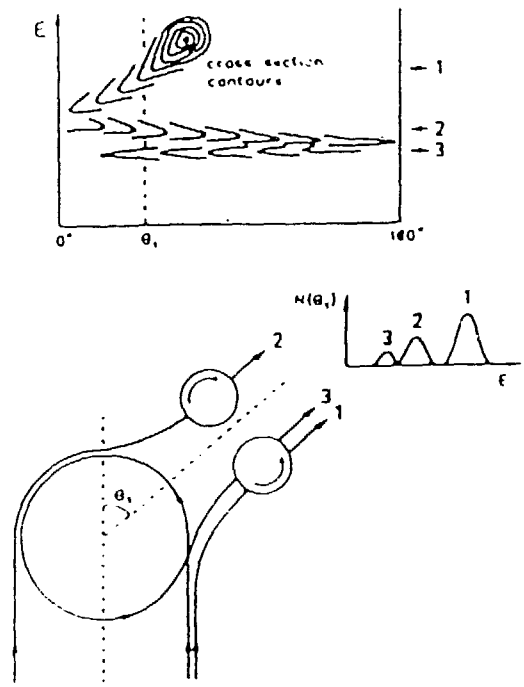

Fi

angles from $^{28}Si+^{12}C$ interactions are shown in Fig. 2. At each bombarding energy the most probable Q-values (peaks) in these spectra showed no dependence on the detection angle. Surprisingly, the angular distributions of these products were found to reflect an isotropic emission probability ($d\sigma/d\Omega \sim 1/\sin\theta$)- this indicates that the dinucleus is spinning very fast or lives very long (or both). Such features make the orbiting indistinguishable from compound nucleus fission, and a small part of that fully damped yield may well be attributable to a fusion-fission process. However, the cross sections measured are more than an order of magnitude larger than ones expected on the basis of conventional Hauser-Feshbach calculations. Other studies of similar yields of binary fragments at backward angles have shown strong memory of the entrance channel [6], and the intermediate lifetimes associated with this process were documented [7]. Studies of spin alignment of the orbiting products [8,9] and the energy division between the outgoing fragments [9,10] have shed additional light on the dynamics of this process and have established it as different from fission of a fully equilbrated compound nucleus.

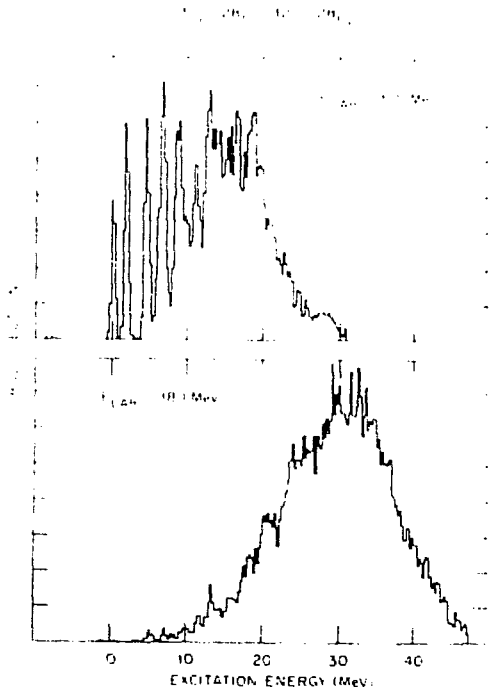

Fig. 2

At each bombarding energy, we can associate a most probable Q-value for any given fragmentation; the dependence of these Q-values on bombarding energy is shown in Fig. 3 for several systems. We have chosen to display the most probable kinetic energies of the fragments, which are derived from the Q-values, and in all cases a

linear dependence is observed at the lower bombarding energies which is then followed by an apparent saturation in the kinetic energies. These results can be interpreted [11] in terms of the formation and decay of a long lived rotating dinuclear complex: the initial (beam's) kinetic energy has been fully damped (converted into excitation of the fragments). Therefore the final kinetic energy of the fragments must equal the sum of potential and rotational energy stored in the rotating complex. The rotational part introduces the linear dependence on bombarding energy, and a simple interpretation of the saturation observed in Fig. 3 stipulates that at some bombarding energy a value of orbital angular momentum is reached, after dissipation, beyond which formation of a dinuclear complex is not allowed due to centrifugal repulsion. The empirical nucleus-nucleus potential in use for describing nucleus-nucleus fusion [12], as shown in Fig. 4, accounts well for the kinetic energy saturation measured for $^{28}Si+^{12}C$.

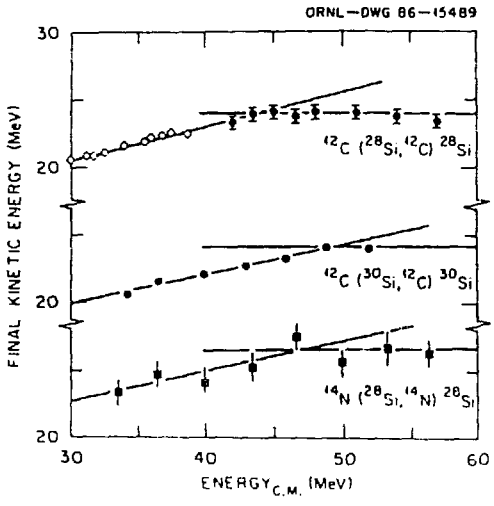

Fig. 3

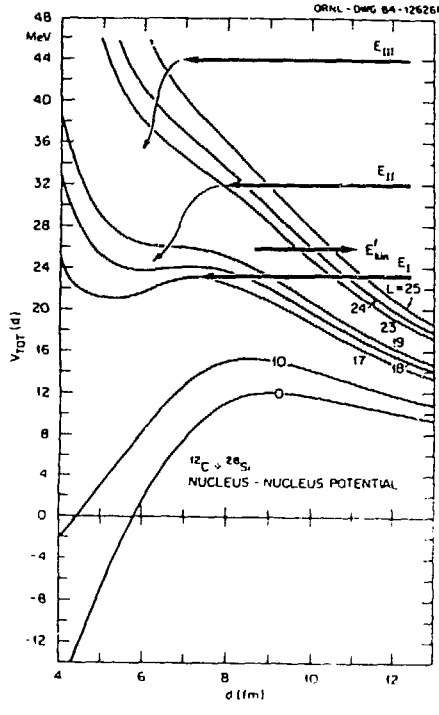

Fig. 4

FUSION DATA

We have postulated that in close collisions between two nuclei a rotating dinuclear complex is formed. We further observe that, due to the finite strength and range of the attractive nuclear forces, a maximum critical angular momentum exists beyond which nucleus-nucleus capture is no more possible. Evidence for a maximum critical angular momentum has also been found in studies of the dependence of the magnitude of the fusion cross section on bombarding energy [13,14]. Using the sharp cutoff approximation (or a variant thereof) one can associate, at any given energy, a maximum angular momentum with the measured cross section. If our interpretation of the orbiting data is correct, the maximum critical angular momentum derived from the fusion data must be bound by the values obtained from analysis of the kinetic energies of fully damped fragments for the same system. We have therefore undertaken a measurement of evaporation residues from fusion of $^{28}Si+^{12}C$ and $^{30}Si+^{12}C$ at bombarding energies as high as 9.5 MeV/A. In the experiment ^{30}Si and ^{28}Si beams from the HHIRF tandem accelerator were used to bombard ^{12}C targets. The compound nucleus formed in these collisions has sufficient momentum to make a full identification of all the products possible (charge by ΔE-E and mass by TOF). The high quality beams available made the measurement of angular distribution to angles as small as 2° (lab) possible. The high quality of the data obtained is evident from Fig. 5. Individual velocity spectra for each outgoing isotope were vital in our data analysis, wherein a comparison of the experimental velocity spectra with the prediction of a statistical evaporation code was used to exclude from our integrated yield any contribution from processes other than fusion-evaporation [15]. Figure 6 shows the critical angular momentum, as derived from the fusion data, for several systems leading to ^{42}Ca and ^{40}Ca [15-19]. The $^{28}Si+^{12}C$ and $^{30}Si+^{12}C$ systems show saturation of the critical angular momentum, and the values are indeed the same as those derived from the kinetic energy saturation in the orbiting data.

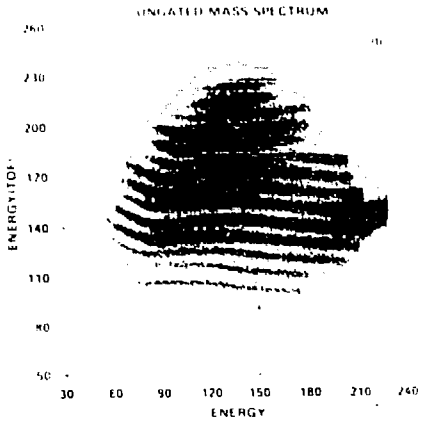

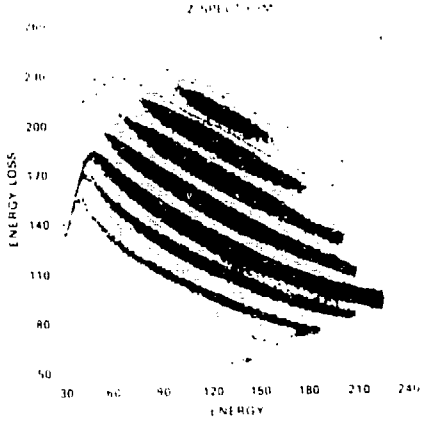

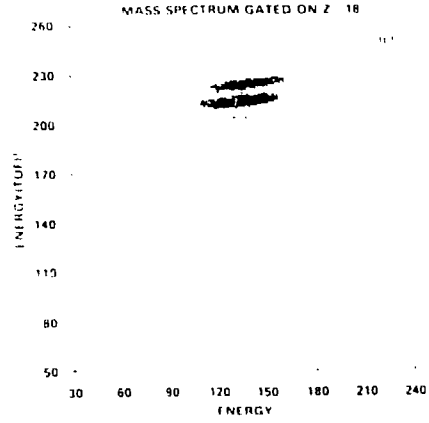

250MeV ^{30}Si + ^{12}C
$\theta_{Lab} = 5°$

TOF, ENERGY AND
ENERGY LOSS RECORDED
EVENT BY EVENT

Fig. 5

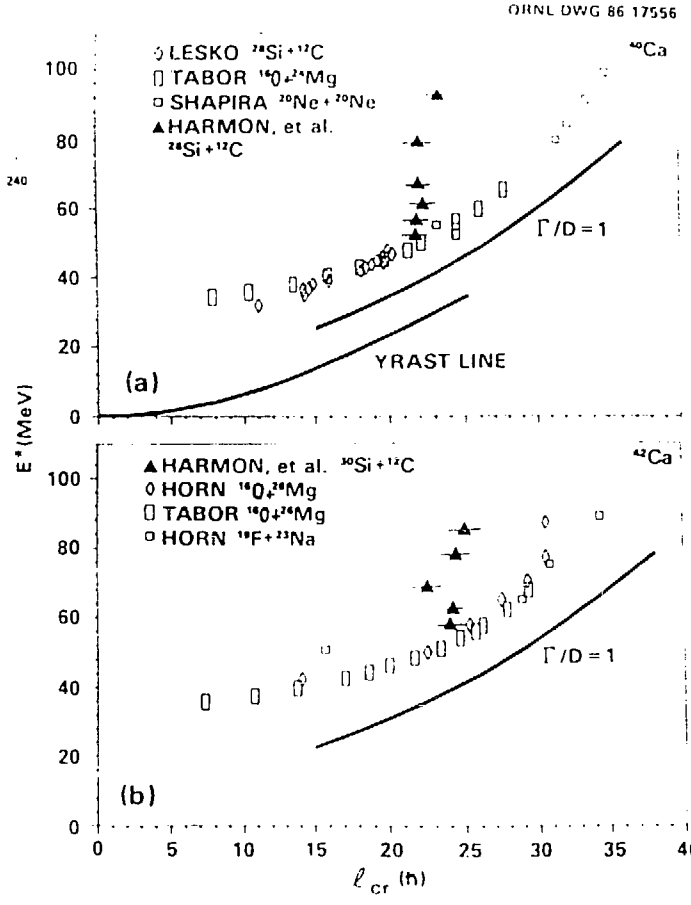

Fig. 6

EQUILIBRATION IN ORBITING

From the data discussed so far, we have concluded that when two nuclei come into close contact, a dinuclear system is formed in the initial stage. This system then undergoes continuous evolution which may lead to binary fragmentation or fusion. The large cross sections for binary fragmentation show that the breakup process competes strongly with fusion. Recently, our work concentrated on trying to understand which degree(s) of freedom is (are) crucial for the transition from orbiting to fusion, or rephrasing that question, what degrees of freedom partake in the local equilibrium which forms the dinuclear stage? It is apparent that the orbiting yield is spread throughout several exit channels; this indicates that the dinucleus evolves via transfer of nucleons between the two clusters forming that system. Does this exchange process reach an equilibrium before the complete fusion into one compound nucleus occurs? The best data pertaining to such a question require the formation of a dinuclear complex via an entrance channel which is not the one most favored on energetic grounds for breakup, and at energies where a large number of exit channels are accessible. Figure 7 shows the potential energies for the ground states of the dinuclear particle transfer channels open to the $^{28}Si+^{12}C$ and $^{28}Si+^{14}N$ interactions. The mass difference (G.S. Q-value) between the entrance channel and each of the other channels has been adjusted by the appropriate difference in the Coulomb, nuclear and centrifugal (ℓ=23) potential energies. Within each particle channel are the channels for inelastic excitation, and these determine the corresponding phase spaces available to each exit channel. It is clear that there are many particle transfer channels accessible to the $^{14}N+^{28}Si$ interaction, even at relatively low excitation energies (this is in stark contrast to the $^{28}Si+^{12}C$ system!). On the basis of energy and phase space considerations, if the duration of orbiting exceeds the time required for charge and mass equilibration, ^{12}C would be the most common product nucleus in the

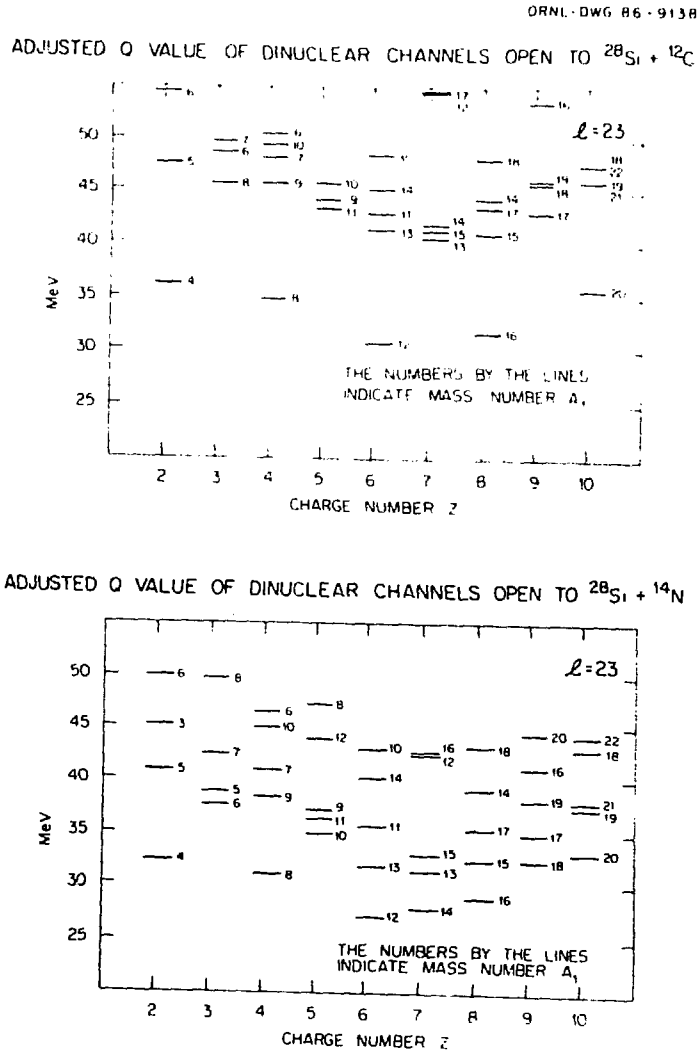

Fig. 7

binary fragmentation following $^{28}Si+^{14}N$ dinuclear formation; otherwise, ^{14}N should be the most abundant. Beams of ^{28}Si from the HHIRF tandem accelerator were used to bombard a ^{14}N supersonic gas jet target - and again in an application of reverse kinematics, recoiling target-like products were detected at forward angles in a magnetic spectrograph. The integrated orbiting yield (assuming isotropic emission at all angles) is shown in Fig. 8 [20]. The ^{12}C

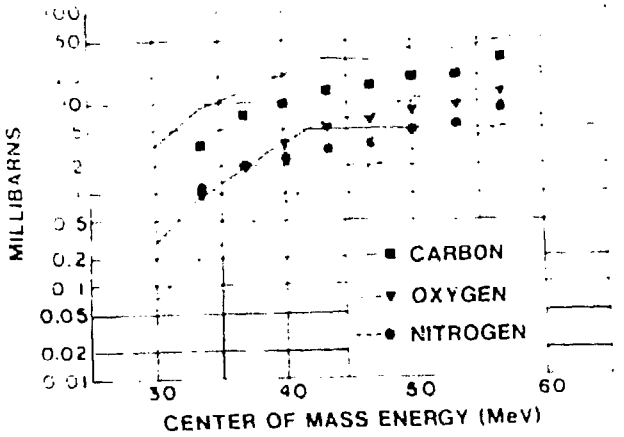

Fig. 3

yields appear dominant over the entire bombarding energy range, indicating a phase space preference in the emission of binary fragments. Also shown are some constrained phase space calculations based on a model that will be described below. These results demonstrate that the rotating dinuclear complex survives long enough for mass and charge exchange to attain local equilibrium before the compound nucleus is formed. What then is the road leading to compound nucleus formation?

DESTINATION FUSION

Fusion could proceed via a continual transfer of charge and mass to the heavy fragment until one nucleus is consumed by the other, or via a continuous evolution from dinuclear to mononuclear shape. In our description of close collisions, the orbiting yield reflects the evolution of the dinuclear complex toward fusion; it seems apt therefore to conclude that fusion occurs through evolution of the shape, since particle transfer has already reached equilibrium during the dinuclear stage. The evolution from the dinuclear, entrance-channel-like to mononuclear shape presumably plays an important role in the evolution of the system toward fusion. We have decided, therefore, to make a detailed comparison of the fusion cross sections for several systems, all leading to the same compound nucleus; fusion data leading to A=40 and A=42 nuclei are available for several systems and have been supplemented

with our data on $^{28}Si+^{12}C$ and $^{30}Si+^{12}C$ (from Fig. 6). Figure 9 shows a collection of all available data on the maximum critical angular momentum limit for fusion plotted as a function of the mass asymmetry in the entrance channel [15-19,21,22]. The critical angular momenta in these systems are presented under two conditions: (1) if the system has shown saturation in the ℓ_{cr} at the highest bombarding energy measured, then we show the maximum ℓ_{cr} with the experimental uncertainty, and (2) if no saturation was observed, we show ℓ_{cr} for the highest bombarding energy as the lower limit on the maximum ℓ_{cr}, and the liquid drop model prediction as the upper limit. The predicted maximum ℓ_{cr} for nucleus-nucleus capture, based on standard, one-term proximity forces and two limiting cases for energy dissipation [12], is also shown in the same figure. It is obvious that such a calculation cannot account for the strong dependence on mass asymmetry of the entrance channel as seen in the data. This should come as no surprise; this difference bears evidence to the fact that nucleus-nucleus capture, which is all the calculation accounts for, cannot in itself describe the high angular momentum limit to fusion and its dependence

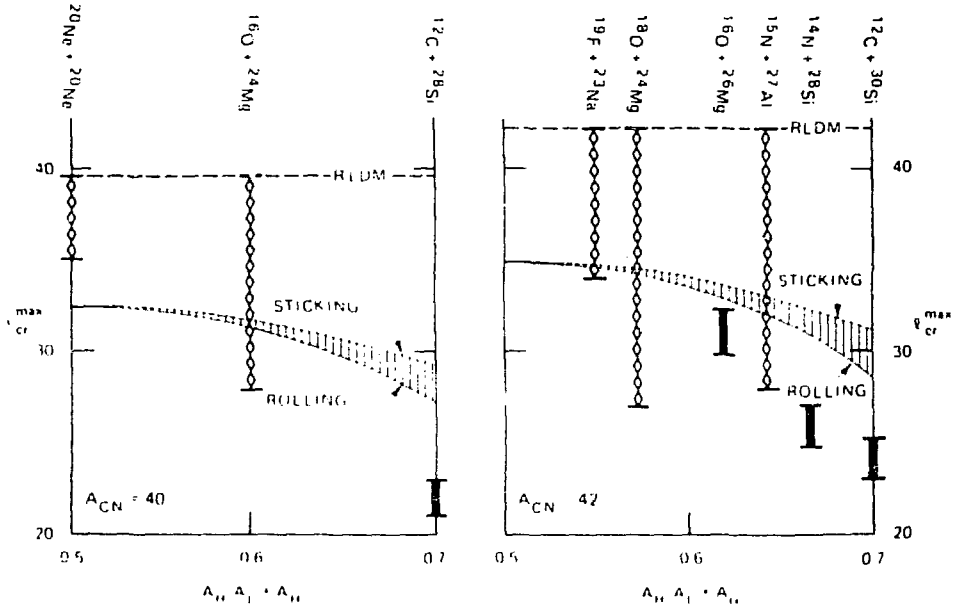

Fig. 9

on mass asymmetry (shape) in the entrance channel. We must emphasize here that, although the road to fusion always involves two steps, it is only at high bombarding energies and angular momenta that the shape transition of the dinuclear complex has a noticeable effect on fusion. Two factors become important at high energy. First is the fact that nucleus-nucleus capture is accompanied by energy dissipation - this opens up possible decay channels for the breakup of the dinucleus - which compete effectively with fusion. The second effect has to do with the change in the saddle configuration of a rotating nucleus. At the higher bombarding energies, the dinuclear complex is formed with high angular momenta; it is well known that the saddle configuration for light nuclei becomes more compact as the spin of that light nucleus increases [23]. At low energies, once nucleus-nucleus capture has occurred, no change in shape is required to reach the saddle configuration, but at high energies, where angular momenta are large, the saddle configuration is far removed from that of two touching spheres. A model description of fusion as a two-step process, therefore, has to incorporate these two ingredients and account for both fusion and orbiting.

A MODEL FOR FUSION AND ORBITING

A pictorial presentation of the process appears in Fig. 10. After dissipation of angular momentum and energy, the incoming nuclei are trapped into forming a rotating dinuclear complex (DMC) which evolves into a fully equilibrated compound nucleus. Throughout

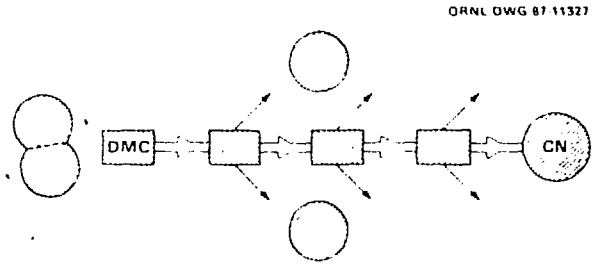

Fig. 10

this evolution, the two clusters in the rotating complex exchange mass and charge. A full description of this continuous exchange of mass and charge in terms of a two-coupled transport equation is required to describe the evolution toward more complex states and the observed breakup into binary fragmentation channels. The competition between breakup and the evolution toward a compound nucleus depends on the energy and angular momentum brought into the system and on the dynamics of the collision process. The transport formalism described in ref. 24 addresses the statistical aspects of the collision. The driving force for particle exchange is the dynamic phase space allocated to the dinuclear and the breakup configurations at each instant. This phase space depends very strongly on the potential energy surface describing each configuration which evolves in time and depends on macroscopic parameters such as the mass and charge of the two clusters, their angular momenta and deformation. The central quantities described by such a model are $\Pi(D,t)$ and $P(C,t)$ - the occupation probabilities for dinuclear and channel states, respectively.

$D \equiv N,Z,E^*,M,\sigma,\ldots$ = set of macroscopic variables defining the dinuclear state,

$C \equiv N,Z,E^*,M,\sigma,\ldots$ = set of macroscopic variables defining the channel state,

where N, Z, E^*, M, σ are neutron and proton numbers, excitation energy, angular momentum projection and deformation (neck).

The data show that the lifetime of the orbiting complex is long enough to bring about full relaxation of the kinetic energies, isotropic emission probability for the fragments, and also equilibration of charge and mass transfer. We therefore calculate a time-independent probability $P_{eq}(C)$ for the dinuclear system to decay into channel C. It is approximated by the density of dinuclear states at the saddle point (the conditional saddle for the particular N,Z partition) and is given by the following expression [24]:

$$P^{\ell}_{eq}(N,Z) = \Pi^{\ell}_{eq}(N,Z) \cdot \frac{\rho[E - U_{\ell}^{sad}(N,Z;R,\sigma)]}{\rho[E - U_{\ell}^{min}(N,Z;R,\sigma)]} \quad (1)$$

Here ρ is the density of states of the dinuclear complex, calculated at R = Rmin (see Fig. 11) and at the saddle point. $\Pi_{eq}(D)$ is the distribution of dinuclear states which is also approximated by the constrained equilibrium distribution of the dinuclear phase space:

$$\Pi^{\ell}_{eq}(D) = \frac{\rho[E - U_{\ell}^{min}(N,Z;R,\sigma)]}{\sum_{N,Z} \rho[E - U_{\ell}^{min}(N,Z;R,\sigma)]} \quad (2)$$

The potential energy surface of the dinuclear complex is a function of mass and charge asymmetry (N,Z) and the collective variables q = (R,σ), (R = distance, σ = deformation, necksize) and is given by the sum of nuclear, Coulomb and centrifugal energies

$$U_{\ell}(N,Z;R,\sigma) = V_n(N,Z;R,\sigma) + V_C(N,Z;R,\sigma) + \frac{\hbar^2\ell(\ell+1)}{2I_{tot}(N,Z;R)} + Q(N,Z) \quad (3)$$

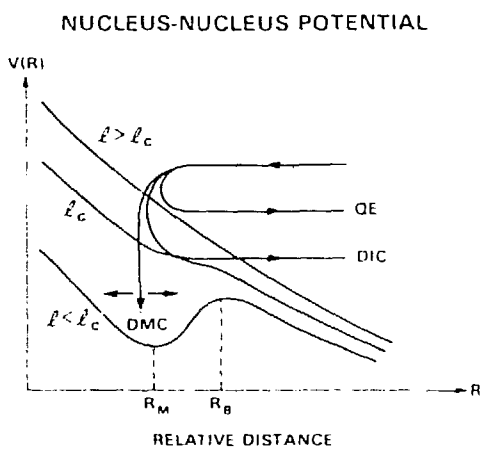

Fig. 11

I_{tot} = total moment of inertia, $Q(N,Z)$ = G.S. Q-value of the fragmentation N,Z with respect to the entrance channel. The entrance channel potential which enters into (2) is the potential energy for two touching spheres given by (3) with no deformation ($\sigma = 0$), often referred to as the "sudden" potential.

Formula (1) has a simple interpretation. It contains two factors; the first factor $\Pi_{eq}(N,Z)$ gives the probability of finding the dinuclear complex with mass and charge asymmetry (N,Z), and the second factor gives the escape probability into the fragmentation channel (N,Z).

Observables can now be calculated using the derived fragmentation probability. The total fragmentation cross section into an exit channel N,Z (orbiting yield) is obtained by summing over all partial waves up to ℓ_{max} which is the maximum angular momentum in the entrance channel that leads to the trapping of the colliding nuclei [15,25]

$$\sigma(N,Z) = \frac{\pi}{k^2} \sum_{\ell=0}^{\ell_{max}} (2\ell + 1)\, P_\ell(N,Z) \tag{4}$$

The total kinetic energy $T_\ell(N,Z)$ of the emitted fragments for each partial wave ℓ is determined by the sum of potential and rotational energies at the conditional saddle (scission) point,

$$T_\ell(N,Z) = U_0^{sad}(N,Z;R,\sigma) + \frac{h^2\ell(\ell + 1)}{2I_{rel}(N,Z;R_S)} f^2 \tag{5}$$

where $I_{rel}(N,Z;R_S)$ is the relative moment of inertia at the saddle point R_S, and $f = I_{rel}(N,Z;R_S)/I_{tot}(N,Z;R_S)$. The potential energy $U_0(N,Z,R,\sigma)$ is given by 3 with $\ell = 0$. The average kinetic energy of the exit channel can then be calculated as

$$T(N,Z) = \frac{\pi}{k^2} \sum_{\ell=0}^{\ell_{max}} (2\ell + 1)\, T_\ell(N,Z)\sigma(N,Z) \,. \tag{6}$$

Since we assume that the dinuclear states which are not fragmented must eventually relax into a compound nuclear configuration, the knowledge of the fragmentation probability [1] allows us to calculate the fusion cross section. For each partial wave, the probability for fusion is determined by $1 - P_\ell$, where P_ℓ is the total fragmentation probability obtained by summing over all possible fragmentations,

$$P_\ell = \sum_{N,Z} P_\ell(N,Z) \quad . \tag{7}$$

Then, the fusion cross section is given as

$$\sigma_f = \frac{\pi}{k^2} \sum_{\ell=0}^{\ell_{max}} (2\ell + 1)[1 - P_\ell] \quad . \tag{8}$$

These results provide a unified and consistent description for the fusion and orbiting processes observed in heavy-ion collisions.

APPLICATIONS

We apply the model developed in the previous section to describe the fusion and orbiting data measured for the system $^{28}Si + ^{12}C$ [24]. For this light system, we expect that deformation will not have an important effect. Therefore, neglecting the neck formation, we represent the equilibrium shape of the DMC for fixed (N,Z) by rigidly rotating two spherical nuclei with a distance R between their centers. Within this approximation, the fragmentation probability [1] takes the form,

$$P_\ell(N,Z) = \frac{\rho[E - U_\ell(N,Z;R_B)]}{\sum_{N,Z} \rho[E - U_\ell(N,Z;R_M)]} \tag{9}$$

where the density of states ρ is evaluated at the top of the barrier ($R = R_B$) and at the minimum ($R = R_M$) (Fig. 11). The potential energy is given by 3 without any neck formation or deformation, $U_\ell(N,Z;R) = U_\ell(N,Z;R,\sigma=0)$. For the density of states, we employ the Fermi gas level density expression [25] with standard level density parameters ($A/8$) and a pairing correction ($\Delta n = \Delta p = 12/\sqrt{A}$ (MeV). In the calculation of the potential energy (3), we chose for the nuclear potential the empirical proximity potential of Bass [14]. The Q-values are obtained from the mass tables and the moments of inertia are approximated by their rigid body values.

The results shown in Figs. 12-14 are spectacular considering the fact that only a small adjustment (<30%) in one of the strength parameters of the potential from ref. 14 was required to describe the kinetic energies, as well as the orbiting and fusion cross sections shown here. Further improvements to the model, such as inclusion of deformation and comparison with data for other systems, will appear in a forthcoming publication.

In summary we have presented data which show that close nucleus-nucleus collisions proceed via the formation of a rotating dinuclear complex toward fusion. The nature of the transition from the dinuclear stage to fusion was elucidated. A model which incorporates mostly statistical aspects of this process has been extremely successful in a quantitative description of the data on $^{28}Si+^{12}C$ collisions.

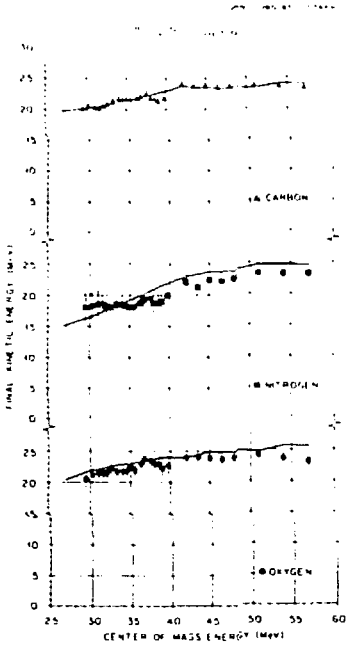

Fig. 12

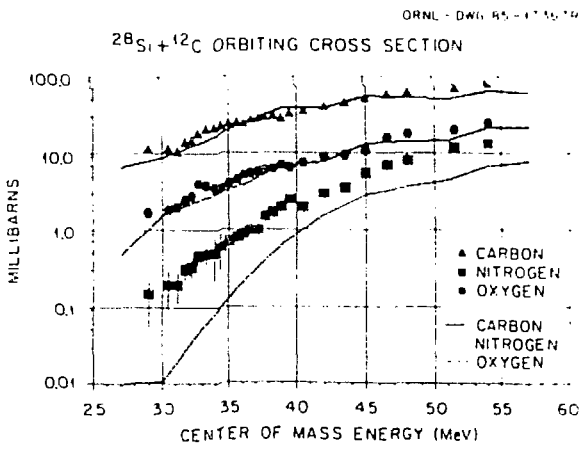

Fig. 13

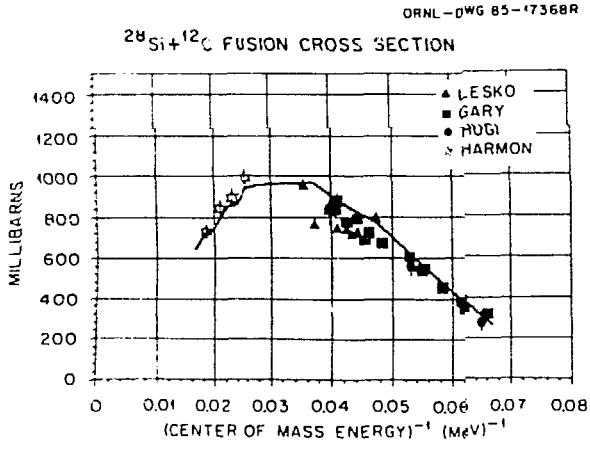

Fig. 14

REFERENCES

1) Huizenga, J. R. and Schroeder, U. W., "Damped Nuclear Reactions", p. 115 vol. 2 of Treatise on Heavy Ion Science, ed. D. A. Bromley Plenum Press 1984. Mosel, U., "Heavy Ion Fusion Reactions", p. 1, ibid.
2) Birkelund, J., et al., Phys. Rep. 56, 107 (1979).
3) Wilczyński J., Phys. Lett. 47B, 484 (1973).
4) Shapira, D., et al., Phys. Rev. Lett. 43, 1781, (1979).
5) Shapira, D., et al., Phys. Lett. 114B, 111 (1982).
6) Ray, A., et al., Phys. Rev. C 31, 1573 (1985).
7) Glaessner, A., et al., Phys. Lett. 169B, 153 (1986).
8) Dunnweber, W., et al., Proc. of 2nd International Conf. on Nucleus-Nucleus Collisions, Visby, Sweden, June 1985, vol. 1, p. 119.
9) Ray, A., et al., Phys. Rev. Lett. 57, 815 (1986).
10) Ray, A., Ph.D. Thesis University of Washington, Seattle, WA.
11) Shapira, D., et al., Phys. Rev. Lett. 53, 1634 (1984).
12) Bass, R., Phys. Rev. Lett. 39, 265 (1977).
13) Gomez del Campo, J., et al., Phys. Rev. Lett. 43, 26 (1979) and Stokstad, R. G., et al., Phys. Lett. 70B, 289 (1977).
14) Morgenstern, H., et al., Z. Phys. A313, 39 (1983).
15) Harmon B. A., et al., Phys. Rev. C 34, 552 (1986) and to be published.
16) Horn, D., et al., Nucl. Phys. A311, 238 (1978); $^{26}Mg+^{16}O$, $^{23}Na+^{19}F$ data.
17) Lesko, K. T., et al., Phys. Rev. C 25, 872 (1982), Jordan, W. J., et al., Phys. Lett. 87B, 38 (1979).
18) Tabor, S. L., et al., Phys. Rev. C 17, 2136 (1978); [$^{16}O+^{24}Mg$, $^{16}O+^{26}Mg$, $^{18}O+^{24}Mg$].
19) Shapira, D., et al., Phys. Rev. C 28, 1148 (1983); [$^{20}Ne+^{28}Ne$].
20) Shivakumar, B., et al., Phys. Rev. Lett. 57, 1211 (1986).
21) Prosser, F. W., et al., Phys. Rev. C 21, 1819 (1980); [$^{15}N+^{27}Al$].
22) Shivakumar, B., et al., to be published and Ph.D. Thesis Yale University.
23) Cohen, S., et al., Ann. Phys. (NY) 82, 557 (1974).
24) Shivakumar, B., et al., Phys. Rev. C 35, 1730 (1987) and Ayik, S., et al., to be published .
25) Bohr, A., Mottelson, B., Nuclear Structure, vol. 1, p. 281, Benjamin, W. A., 1969.

DISCLAIMER